

Supplementary Information

Theranostic near-infrared fluorescent nanoplatform for imaging and systemic siRNA delivery to metastatic anaplastic thyroid cancer

Yanlan Liu^{a§}, Viswanath Gunda^{b§}, Xi Zhu^a, Xiaoding Xu^a, Jun Wu^a, Diana Askhatova^a, Omid C.
Farokhzad^{*a}, Sareh Parangi^{*b}, and Jinjun Shi^{*a}

^aDepartment of Anesthesiology, Brigham and Women's Hospital, Harvard Medical School, Boston, MA, 02115, USA

^bDepartment of Surgery, Massachusetts General Hospital, Harvard Medical School, Boston, MA 02214, USA

[§]These authors contributed equally to this work.

*To whom correspondence should be addressed. E-mail: jshi@bwh.harvard.edu (J.S.), sparangi@partners.org (S.P.), or ofarokhzad@bwh.harvard.edu (O.C.F.)

Contents:

1. Methods
2. Supplementary Figures 1-16 and Figure Legends
3. References

Materials

polyPCPDTBT and ethylenediamine core-poly (amidoamine) (PAMAM) generation 0 dendrimer (G0) were purchased from Sigma-Aldrich. DSPE-PEG (1,2-distearoyl-*sn*-glycero-3-phosphoethanolamine-N-[methoxy(polyethylene glycol)]) with PEG molecular weight 3000 (DSPE-PEG3k) was obtained from Avanti Polar Lipids. The Steady-Glo luciferase assay system was purchased from Promega. siRNAs targeting luciferase (siLuc) and BRAF (siBRAF) and fluorescent dye-labeled siRNAs were custom-synthesized by Dharmacon. The siRNA sequences are shown in Supplementary Table 1. LysoTracker Green (Life Technologies) was resuspended in dimethyl sulfoxide (DMSO; Sigma) and used at a final concentration of 200 nM. Alexa Fluor 488 phalloidin was purchased from Life Technologies. Antibodies used in this work are from Cell Signaling and Santa Cruz Biotechnology, Inc.

Synthesis and characterization of siRNA-encapsulated NIR NPs

The cationic lipid was synthesized according to a method previously described (1). In a typical synthesis of the siRNA-encapsulated NIR NPs with negative charges, 0.5 nmol siRNA in 5 μ L of water was added into 500 μ L of THF mixture solution containing polyPCPDTBT (0.25 mg/mL), GO-C14 (0.125 mg/mL), and DSPE-PEG3k (0.5 mg/mL). Next, this mixture was added dropwise into 5 mL water under vigorous stirring and kept at room temperature for 1 hour. Next, NPs were collected, washed with water twice using Amicon tubes (MWCO 100kDa; Millipore) at 4 °C, and finally resuspended in phosphate-buffered saline (PBS) solution.

The size and surface charge (zeta potential) of NPs were determined by Dynamic Light Scattering or DLS (15-mW laser, incident beam of 676 nm; Brookhaven Instruments Corporation). The morphology of NPs was characterized using a Tecnai G2 Spirit BioTWIN microscope (FEI Company) operating at 80 kV.

Release kinetics of siRNA from NPs

To determine the release kinetics, dye-labeled siRNA was incorporated into three NP formulations with different surface charges. The suspension of NPs in PBS was added in semipermeable mini dialysis tubes (MWCO 100 kDa; Pierce) and dialyzed against PBS (pH 7.4) at 37 °C with gentle stirring. At the indicated time interval, an aliquot of the NP suspension was removed, and the fluorescence intensity of the dye was measured using the Synergy HT multi-mode microplate reader (BioTek Instruments Inc.).

Cell culture

Luciferase-expressing HeLa (Luc-HeLa) cells, BRAF^{V600E}-mutated 8505C, SW1736, and BCPAP thyroid cancer cells were cultured in RPMI-1640 medium (ATCC) supplemented with 10% (v/v) FBS with high glucose. All cells were maintained at 37 °C in 5% CO₂ and a humidified atmosphere.

***In vitro* luciferase silencing**

For the silencing experiments, Luc-HeLa cells were seeded into 96-well plates (3,000 cells per well) and allowed to attach for 24 hours at 37°C in 5% CO₂ and a humidified atmosphere. Then the cells were treated with NIR NPs loaded with siRNA against luciferase (NP(siLuc)) at different concentrations and incubated for 48 hours. The medium was then changed, and the cells were cultured for another 24 hours. The expression of firefly luciferase in control cells and NP(siLuc)-treated cells was determined using Steady-Glo luciferase assay kits (Promega) according to the manufacture's instructions. Cell number and the cytotoxicity of nanoparticles were quantified using the AlamarBlue assay. All the *in vitro* transfection experiments were performed in triplicate.

***In vitro* cell proliferation**

Alamar Blue assay was performed to evaluate cell proliferation (it is non-toxic and has no impact on cell proliferation). Briefly, BRAF^{V600E}-mutated 8505C cells were plated and cultured in 6-well tissue culture plates at a density of 10,000 cells/well for 24 hours. The cells were then transfected with NP(siControl) or NP(siBRAF) for another 24 hours. At different time intervals, cells were quantified by Alamar Blue assay according to the manufacturer's instructions. siRNA targeting luciferase was used as the control siRNA for all control groups.

***In vitro* invasion, migration, and adhesion assays**

Invasion assays were performed using 24-well BioCoat Matrigel invasion chambers according to the manufacturer's instructions (BD Biosciences). In brief, 72 h after treatment of NP (siBRAF) and NP (siControl), cells were counted and transferred to the chambers at a density of 50×10^3 cells/mL in serum-free medium with 5% FBS in growth medium as a chemoattractant. After incubation for 24 hours, the non-invading cells were removed from the chambers and the membrane was carefully washed. The cells trapped in the membrane were stained with Hoechst and quantified under the microscope. Migration assays were conducted for 24 hours in culture with chambers that did not contain Matrigel (Corning) according to the manufacturer's instructions. Cell adhesion was tested using 96-well cell-culture plates (Life Technologies) coated with type I collagen, with BSA-coated plates as control. After incubation for 2 hours at 37°C, the plates were washed, and the cells adhering to the bottom of the well were fixed for counting. For all assays, cells were counted (per field), and five fields were chosen per insert for invasion and migration assays, or per well for cell adhesion assay.

Western blot analysis

Protein extracts were prepared using modified radioimmunoprecipitation assay lysis buffer (50 mM Tris-HCl pH 7.4, 150 mM NaCl, 1% NP-40 substitute, 0.25% sodium deoxycholate, 1 mM

sodium fluoride, 1 mM Na₃VO₄, 1 mM EDTA), supplemented with protease inhibitor cocktail (Cell Signaling) and 1mM phenylmethanesulfonyl fluoride. Equal amounts of protein, as determined with a bicinchoninic acid (BCA) protein assay kit (Pierce/Thermo Scientific) according to the manufacturer's instructions, were resolved on SDS-PAGE gels and transferred to nitrocellulose or polyvinylidenedifluoride membrane. The blots were blocked with 3% BSA in TBST (50 mM Tris-HCl, pH 7.4 and 150 mM NaCl, and 0.1% Tween 20) and then incubated with appropriate primary antibodies overnight at 4 °C. Signals were detected with horseradish peroxidase-conjugated secondary antibodies and an enhanced chemiluminescence (ECL) detection system (Pierce).

Immunofluorescence staining

For immunofluorescence experiments, after treatment of NP(siControl) or NP(siBRAF), the cells were washed with PBS and fixed with 4% paraformaldehyde at room temperature for 15 min. Following washing with PBS for three times (5 min each), the cells were permeabilized by incubation in 0.2% Triton X-100 in PBS for 5 minutes on ice, followed by washing with PBS twice (5 min each). Thereafter, the cells were blocked with blocking buffer (2% normal goat serum, 2% BSA, and 0.2% gelatin in PBS) at room temperature. After 1 hour, the cells were washed with PBS three times (5 min each) and incubated with appropriately diluted BRAF antibody for 1 hour at room temperature, rinsed with PBS three times, and incubated with diluted fluorescent dye-linked secondary antibody and dye-labeled phalloidin (Life Technologies) for another hour. After washing with PBS, the cells were stained with Hoechst 33342, and finally mounted on slides with Prolong Gold antifade mounting medium (Life Technologies). The fluorescence images were obtained using a Leica DM-IRE2 inverted fluorescence microscope (Leica Microsystems).

Immunohistochemistry staining

Immunohistochemistry staining was performed on formalin-fixed paraffin-embedded tumor sections. Briefly, tumor slides were first heated to 60°C for 1 hour, desparaffinized with xylene three times (5 min each), and washed with different concentrations of alcohol. After retrieval of antigen using DAKO target retrieval solution at 95-99 degrees for 40 min, followed by washing, the slides were blocked with peroxidase blocking buffer (DAKO Company) for 5 min. After being washed with washing buffer (DAKO Company), the slides were incubated with primary antibody solution (diluted in DAKO antibody diluent) for 1 hour. The slides were then washed again and incubated with peroxidase-labeled polymer for 30 min. After washing, the slides were stained with DAB+ substrate-chromogen solution and hematoxylin. Finally, the slides were mounted and imaged using MVX10 MacroView Dissecting scope equipped with an Olympus DP80 camera.

Animals

Animals were provided by the Charles River Laboratories. Animal care and handling procedures were in accordance with National Institutes of Health animal care guidelines for all *in vivo* experiments. Animal protocols were approved by the Institutional Animal Care and Use Committees on Animal Care (Harvard Medical School). The animals were allowed free access to sterile food pellets and water.

Pharmacokinetic study

For *in vivo* pharmacokinetic study of the NIR polymer nanoparticles, healthy C57BL/6 mice were intravenously injected with different NIR NPs through the tail vein. At different time points, blood was collected by a retro-orbital puncture and the fluorescence of polymer in the blood was measured using the BioTekmicroplate reader.

ATC tumor models

For the xenograft tumor models, BRAF^{V600E}-mutated 8505C cells were cultured in RPMI-1640 supplemented with 10% FBS at 37 °C in an atmosphere of 5% CO₂ and 95% air. For the ATC tumor xenograft model, 2×10⁶ BRAF^{V600E}-mutated 8505C cells were suspended in 200 μL of 50% Matrigel (BD Matrigel™) with serum-free culture medium (1:1 v/v%) and then inoculated subcutaneously into the bilateral flanks of 4-week-old female athymic nude mice. The mice were used for further experiments when the tumors had grown to 5-10 mm in diameter.

In vivo orthotopic thyroid cancer models were set up according to a previously described procedure (2). In brief, female severe combined immunodeficiency (SCID) mice 4-6 weeks old were first anesthetized using 200 μL of a mixture of ketamine (90 mg/mL) and xylazine (10 mg/mL). 5× 10⁵ BRAF^{V600E}-mutated 8505c cells suspended in 10 μL of serum-free RPMI medium were injected into the right thyroid using a Hamilton syringe (Fisher Scientific) linked to a 27-gauge standard needle. After the injection, the incision was closed using two or three interrupted 3-0 nylon sutures, and the mice were then placed under a warming lamp until they recovered from anesthesia.

Biodistribution and *in vivo* NIR imaging

For the *in vivo* biodistribution study, female athymic nude mice bearing BRAF^{V600E}-mutated 8505C xenografts and female SCID mice implanted with orthotopic thyroid tumors were intravenously injected with NIR polymer nanoparticles through the tail vein. Twenty four hours after administration, mice were imaged using the SyngenePXi imaging system (Synoptics Ltd). Organs and tumors were also harvested and imaged for qualification.

For time-dependent tumor imaging, the female athymic nude mice bearing the BRAF^{V600E}-mutated 8505C xenograft received a single injection of NIR NPs, and whole-body NIR fluorescence was imaged using the Syngene PXi imaging system under irradiation of 740 nm.

To evaluate the capability of NIR NPs in sentinel lymph node mapping, healthy female athymic nude mice were subcutaneously administered NIR nanoparticles into forepaws, and NIR fluorescence in sentinel lymph nodes was monitored after 10 min postinjection. For systemic lymph node imaging, healthy female athymic nude mice were intravenously administered NIR NPs through the tail vein. At 24 h postinjection, the axillary lymph nodes, inguinal lymph nodes, neck lymph nodes, and lateral thoracic lymph nodes were harvested for NIR imaging with a small piece of muscle as a reference.

***In vivo* therapeutic efficacy and inhibition of tumor metastases**

The tumor growth-inhibitory effect of NP(siBRAF) was evaluated in both BRAF^{V600E}-mutated 8505C xenograft tumor models and *in vivo* orthotopic thyroid cancer models. Mice were randomly divided into three treatment groups (4 per group for xenograft tumor models, 6 for *in vivo* orthotopic thyroid cancer models). For xenograft tumor models, when the tumor size reached 50-100 mm³, different regimens including (i) PBS, (ii) NP(siControl), and (iii) NP(siBRAF) were administered intravenously at a dose of 600 µg siRNA per kilogram of animal weight every other day three times. Tumor size in the xenograft tumor model was measured by caliper every other day, and tumor volume was calculated as: volume = tumor length × (tumor width)² / 2. Relative tumor volumes were calculated as V/V₀ (V₀ was the tumor volume when the treatment was initiated).

For the *in vivo* orthotopic tumor model, 2 weeks after injection of BRAF^{V600E}-mutated 8505C cells into the thyroid gland, the mice were randomly divided into three groups (6 mice each) and

then injected with PBS, NP(siControl), or NP(siBRAF) at a dose of 600 µg siRNA per kilogram of animal weight every other day five times. One month later, the mice were sacrificed and their necks opened for imaging. The tumor volume was calculated with the method discussed above.

For metastasis study, 2 weeks after injection of BRAF^{V600E}-mutated and GFP-expressing 8505C cells into the thyroid gland, the mice were randomly divided into two groups (3 mice each) and injected with NP(siControl) or NP(siBRAF) at a dose of 600 µg siRNA per kilogram of animal weight every other day five times. One month later, the mice were sacrificed, and the metastases in the lungs were evaluated with both fluorescence and IHC staining.

Hematologic examination and histology

For the *in vivo* toxicity study, healthy C57BL/6 mice were administered 3 daily intravenous injections of (i) saline, (ii) naked siBRAF, (iii) NP(siControl), or (iv) NP(siBRAF), at 600µg siRNA/kg animal. Blood was collected by a retro-orbital puncture, serum separated for blood biochemistry assay, and the organs were harvested, fixed in a 10% formalin solution, and embedded in paraffin for H&E staining.

To test the blood biocompatibility of nanoparticles, red blood cells were collected after centrifugation at 2000 g/min for 10 min. After washing with PBS five times, red blood red cells were diluted x10 with PBS. Thereafter, 0.1 mL of red blood cell solution was added into 0.4 mL of PBS containing different concentrations of NPs, PBS alone (negative control), and deionized water (positive control), respectively. After incubation at room temperature for 3 hours, the samples were centrifuged at 14,800 rpm/min for 30 min. The absorbance of the supernatants at the wavelength of 541 nm was examined using a microplate reader. The hemolysis of NPs was calculated according to the following equation:

$$\text{Hemolysis\%} = (A_{\text{sample}} - A_{(-)\text{control}}) / (A_{(+)\text{control}} - A_{(-)\text{control}})$$

A represents the absorbance of the sample at the wavelength of 541 nm.

Immune response

C57BL/6 mice were intravenously administered a single dose of PBS, naked siBRAF, blank NP, or NP(siBRAF). 24 hours after injection, blood was collected and serum isolated for measurements of representative cytokines (TNF- α , IL-6, IL-12, and IFN- γ) by enzyme-linked immunosorbent assay or ELISA (PBL Biomedical Laboratories and BD Biosciences) according to the manufacturer's instructions.

Statistical analysis

All data are presented as their means with S.D., unless otherwise noted. Statistical significance was determined by a two-tailed Student's t test assuming equal variance. A p value <0.05 is considered statistically significant. Statistical values are indicated in figures according to the following scale: * = $p < 0.05$ and ** = $p < 0.01$.

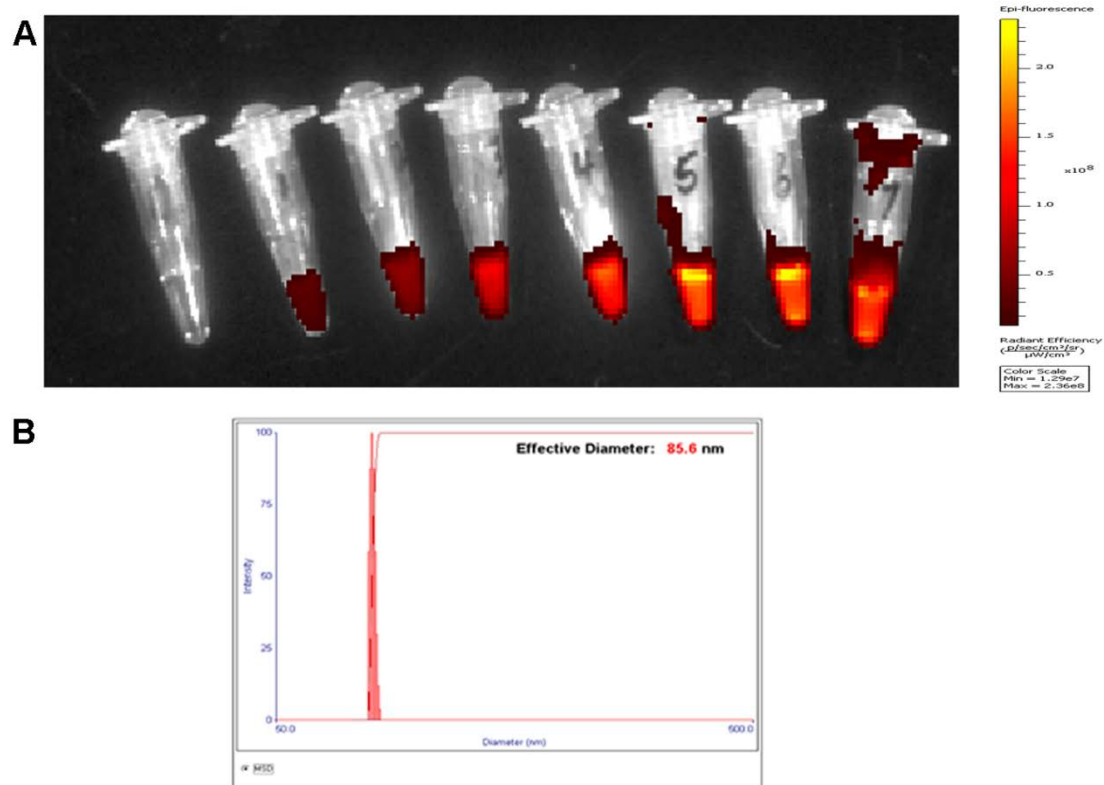


Fig. S1. Characteristics of NIR NPs. (A) NIR fluorescence of NIR NPs upon irradiation at 710 nm. (B) The hydrodynamic size of NIR NPs determined by dynamic light scattering (DLS).

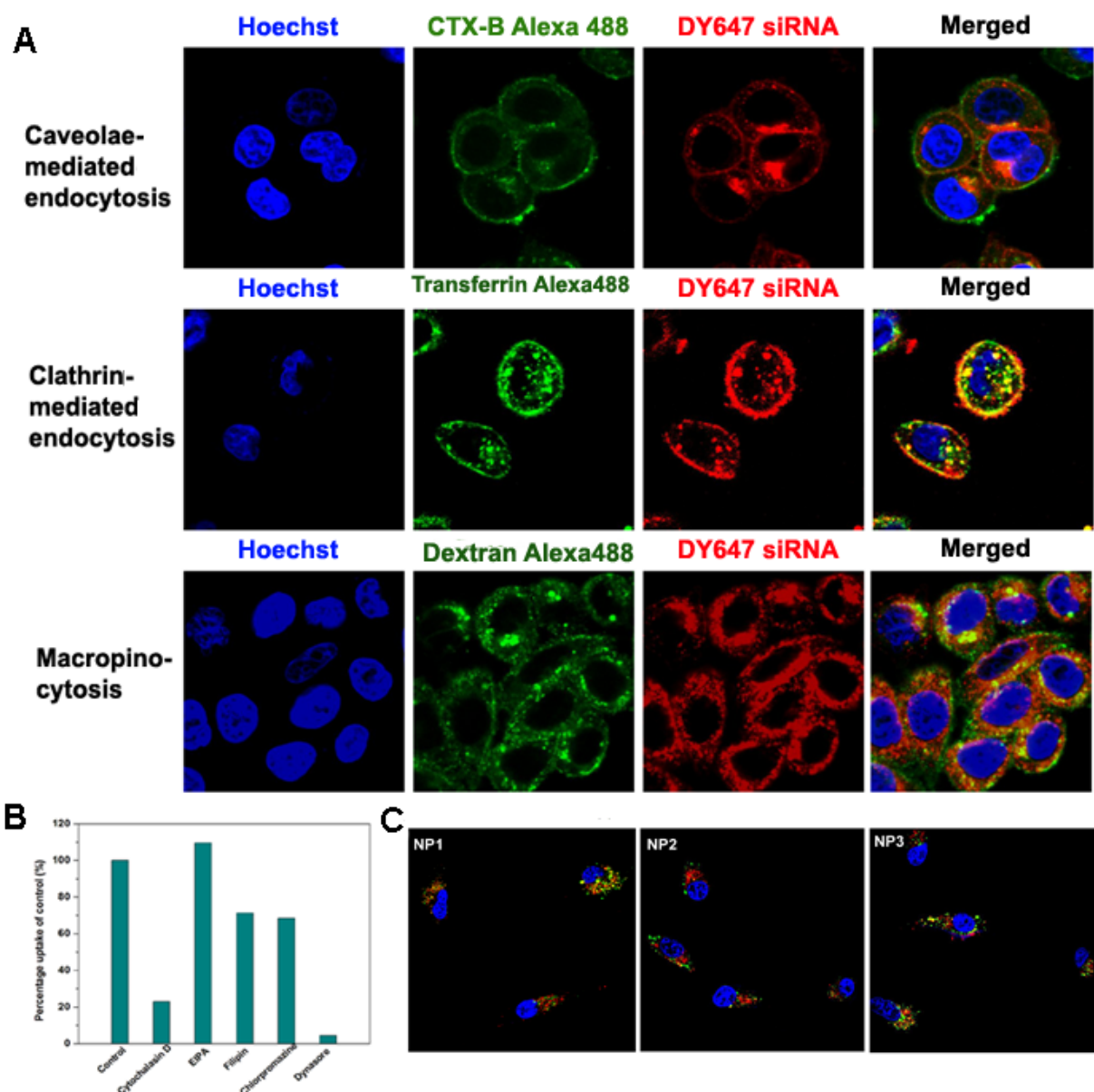


Fig. S2. Endocytotic pathway and endosomal escape of siRNA from NPs. (A) Confocal imaging of fluorescent markers of different endocytosis pathways. The biomarkers are: dextran for macropinocytosis, CTX-B for caveolae-mediated endocytosis, and transferrin for clathrin-mediated endocytosis. (B) NP uptake in HeLa cells treated with different inhibitors based on flow cytometry. (C) Confocal imaging of HeLa cells after incubation of three types of NIR NPs for 4 h. The endosomes are labeled with LysoTracker Green.

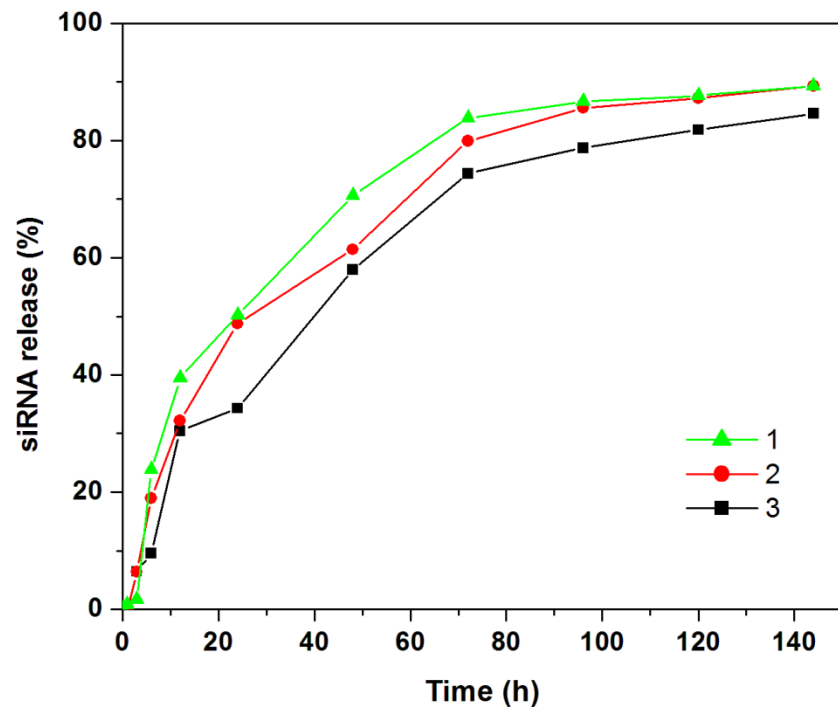


Fig. S3. siRNA release profiles from three NPs with different surface charges. 1: NP#1, 2: NP#2, and 3: NP#3.

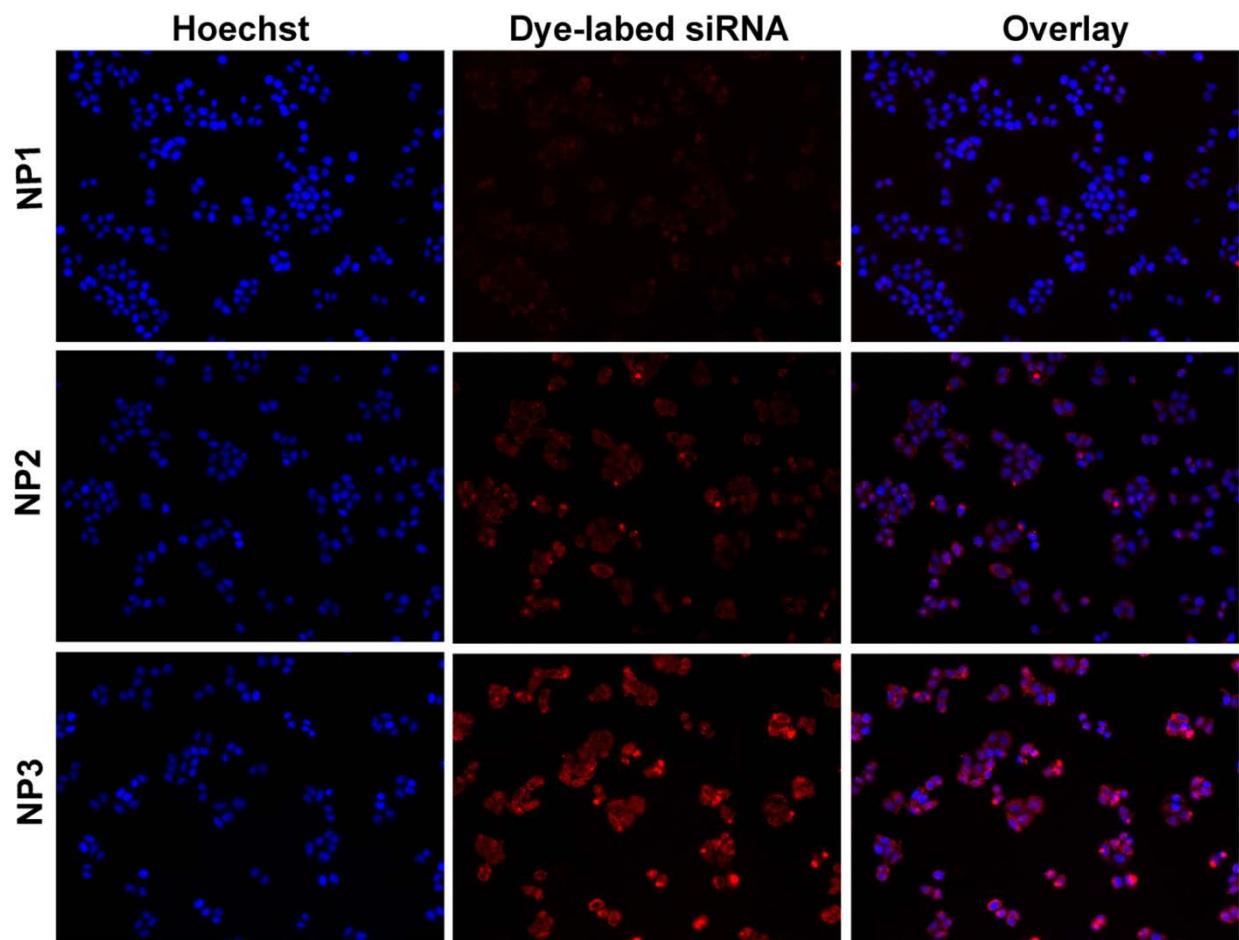


Fig. S4. Uptake of NPs with different surface charges in HeLa cells after 12 h of incubation. NP#1, NP#2, and NP#3.

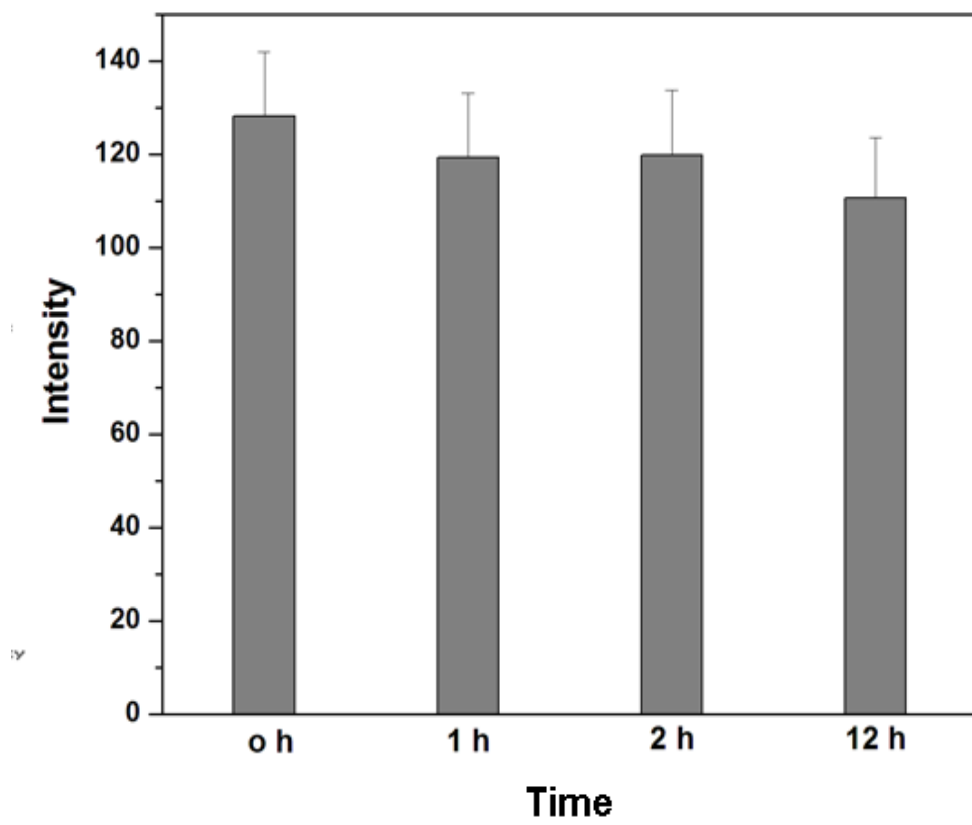


Fig. S5. Photostability of NIR NPs under laser irradiation.

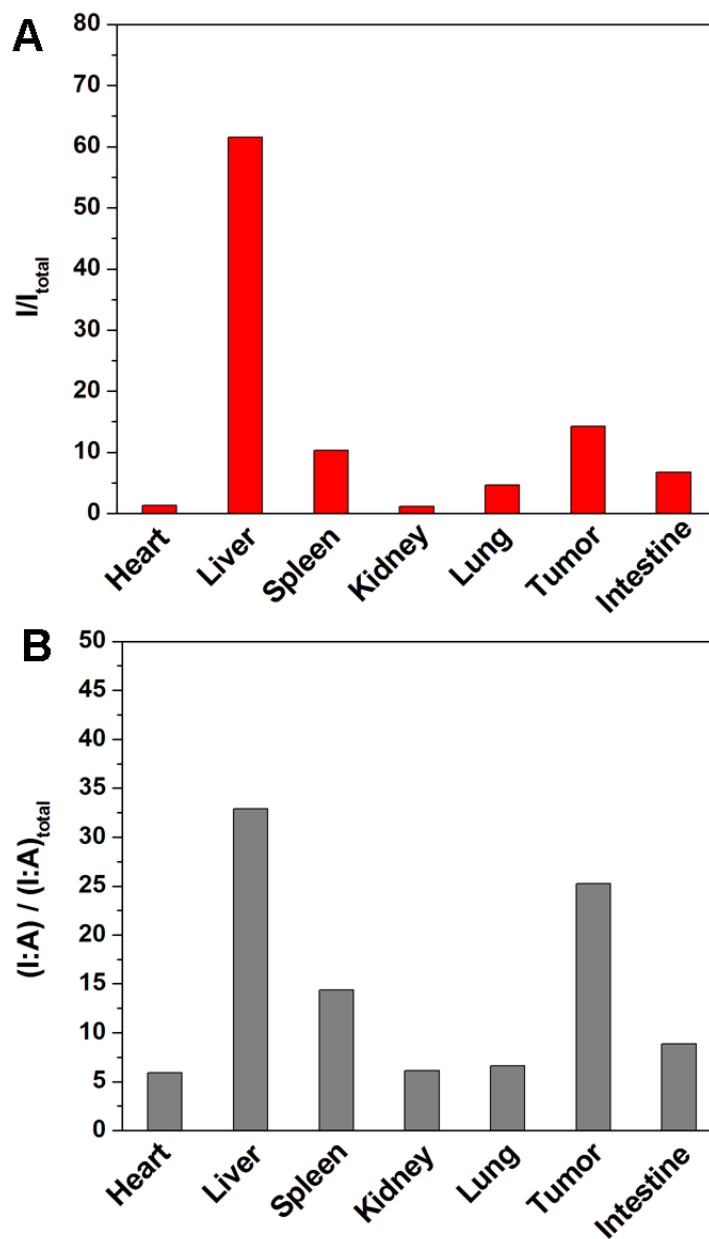


Fig. S6. Biodistribution of NIR NPs in the xenograft ATC model. (A) NIR fluorescence of organs from BRAF^{V600E}-mutated 8505C tumor-bearing mouse at 24 h postinjection of NIR NPs. (B) Quantitative biodistribution analysis from (A), where I is the fluorescence intensity of the organ, and A is the area of the organ.

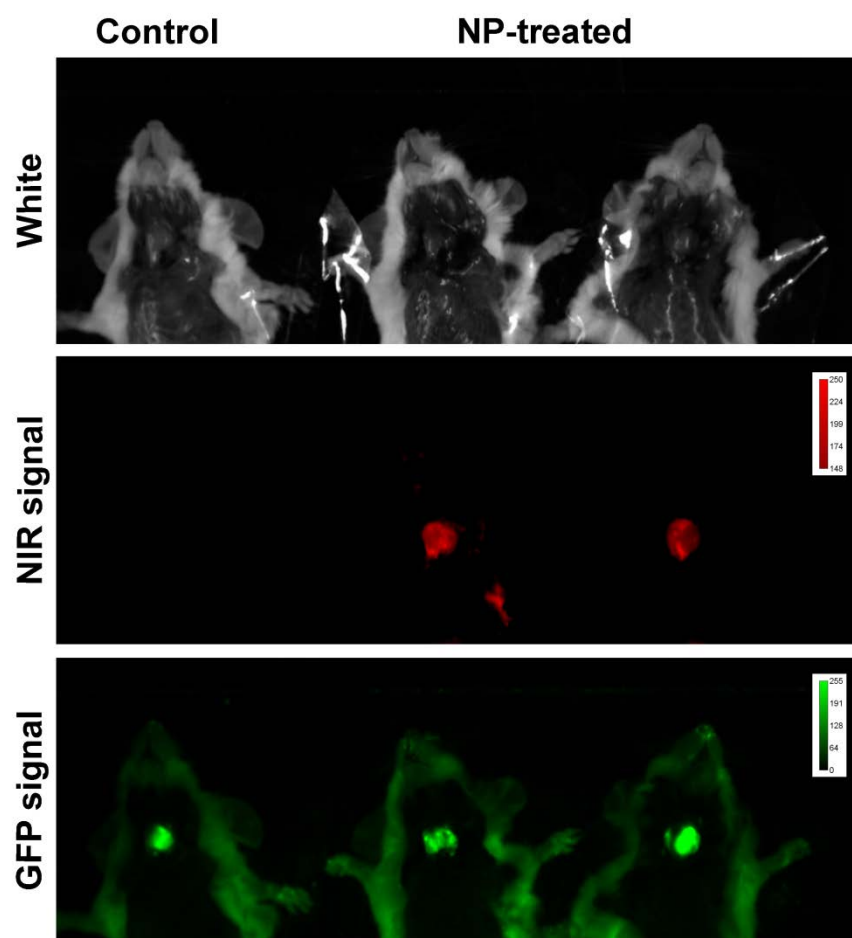


Fig. S7. *In vivo* NIR fluorescent imaging in the orthotopic ATC model following treatment with NIR NPs. 8505C cells harboring BRAF^{V600E} and expressing green fluorescent protein (GFP) were used for tumor implantation.

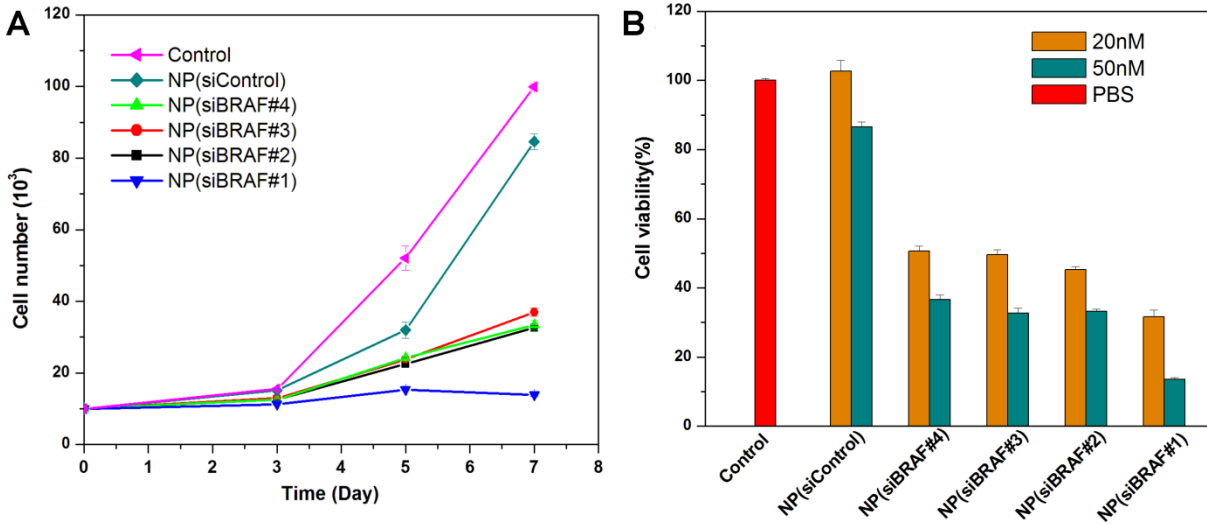


Fig. S8. Cell proliferation of BRAF^{V600E} mutated 8505C cells after treatment with NP(siControl) or NP (siBRAF) with different siBRAF sequences at a higher concentration of si(BRAF).

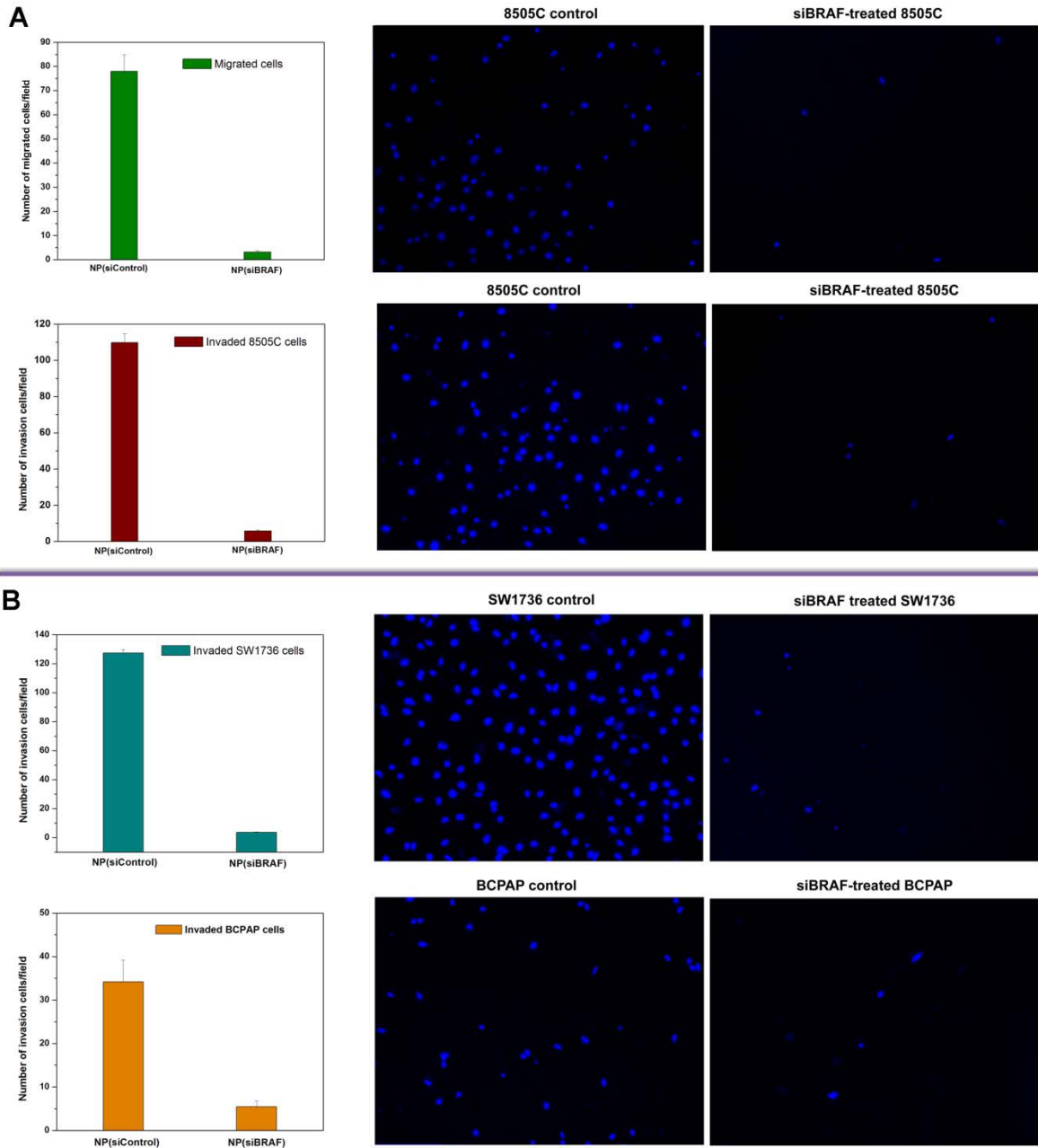


Fig. S9. Inhibition effects of NP(siBRAF) on the invasion and migration of thyroid carcinoma cells. (A) Number and fluorescence images of the invaded or migrated 8505C cells, (B) Number and fluorescence images of invaded SW1736 and BCPAP cells following treatment with NP(siControl) or NP(siBRAF). The cells are stained with Hoechst 33342.

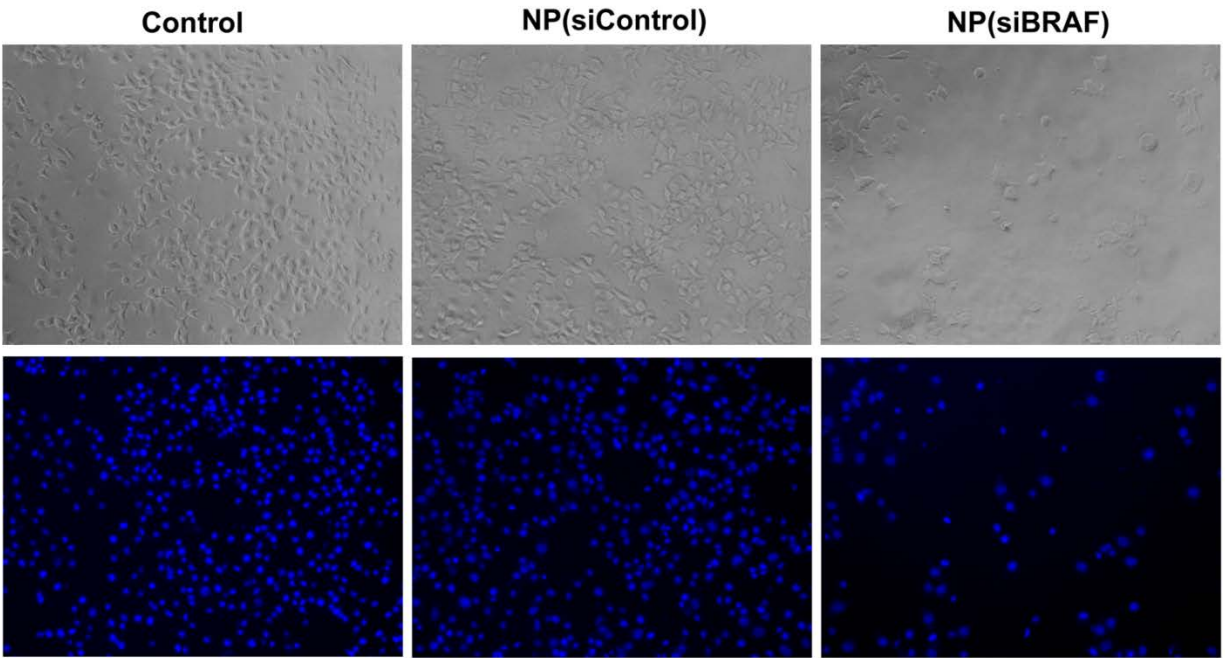


Fig. S10. *In vitro* cell adhesion assay. Knockdown of BRAF by NP(siBRAF) reduces the number of BRAF^{V600E}-mutated 8505C cells that adhered to type I collagen as compared to non-treated or NP(siControl) treated cells.

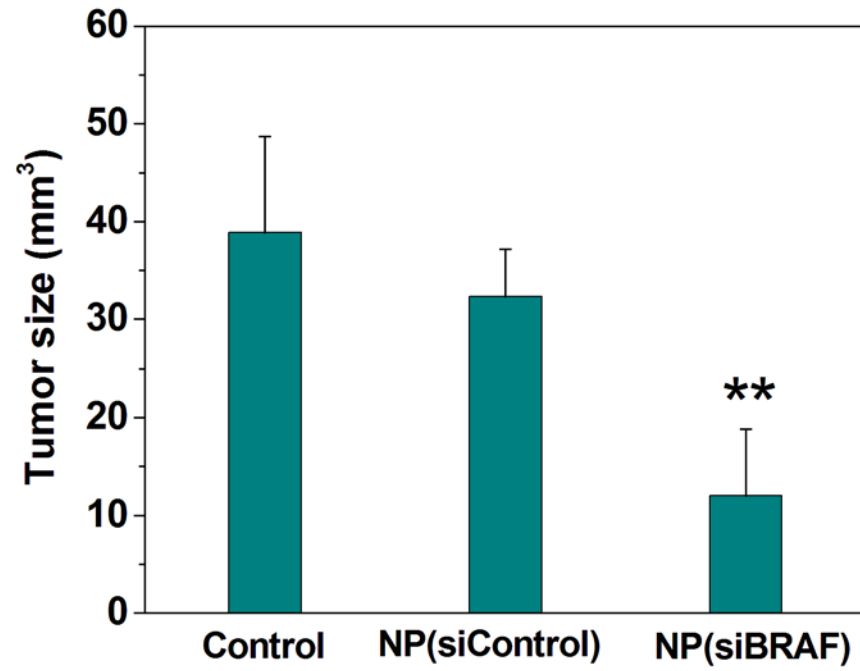


Fig. S11. Therapeutic efficacy of NP(siBRAF) in orthotopic ATC mouse models. (** $p < 0.01$ vs. Control and NP(siControl)).

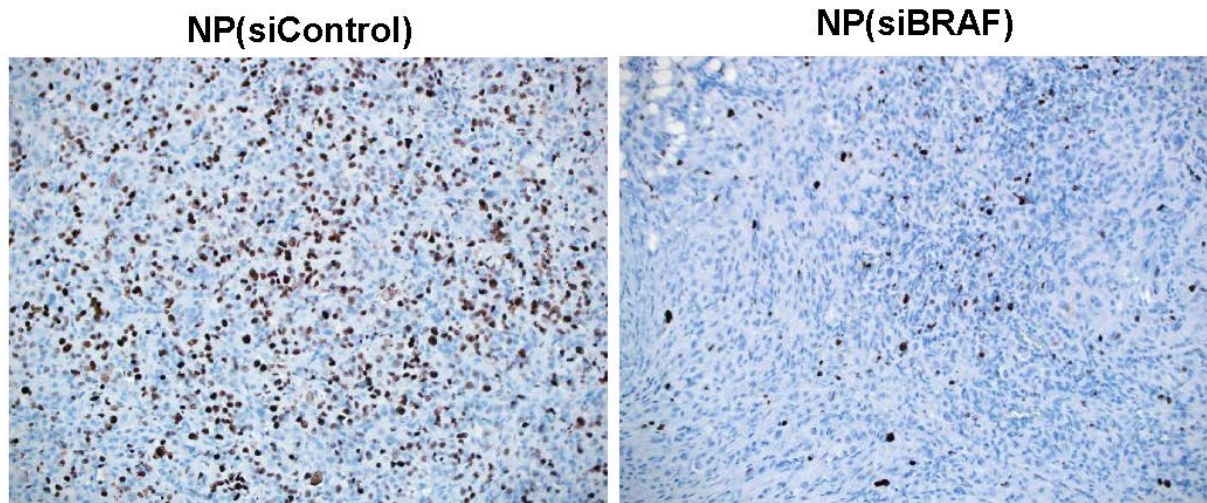


Fig. S12. IHC staining of Ki67 in the tumor tissues of mice treated with NP(siControl) or NP(siBRAF).

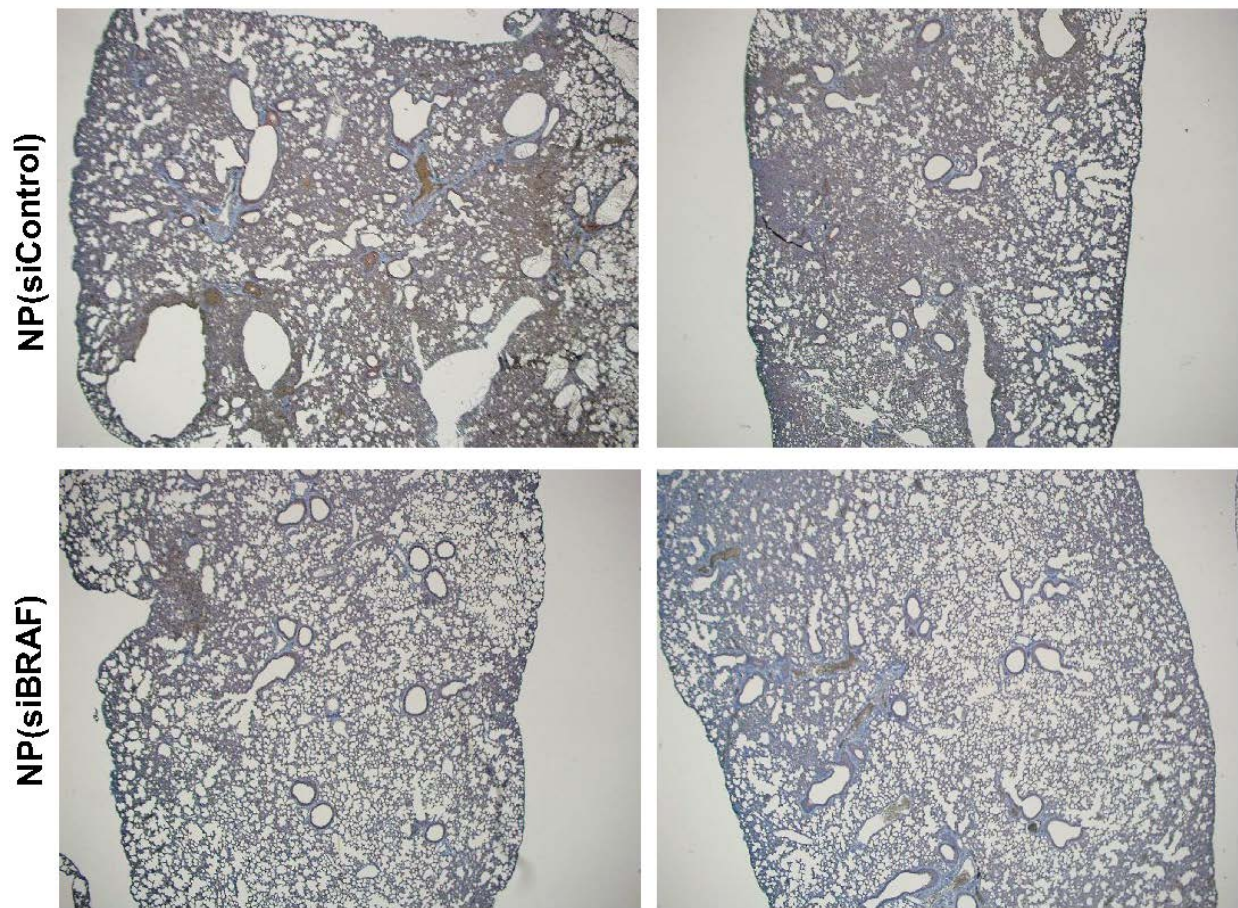


Fig. S13. IHC staining of BRAF in the lungs of mice treated with NP(siControl) or NP(siBRAF).

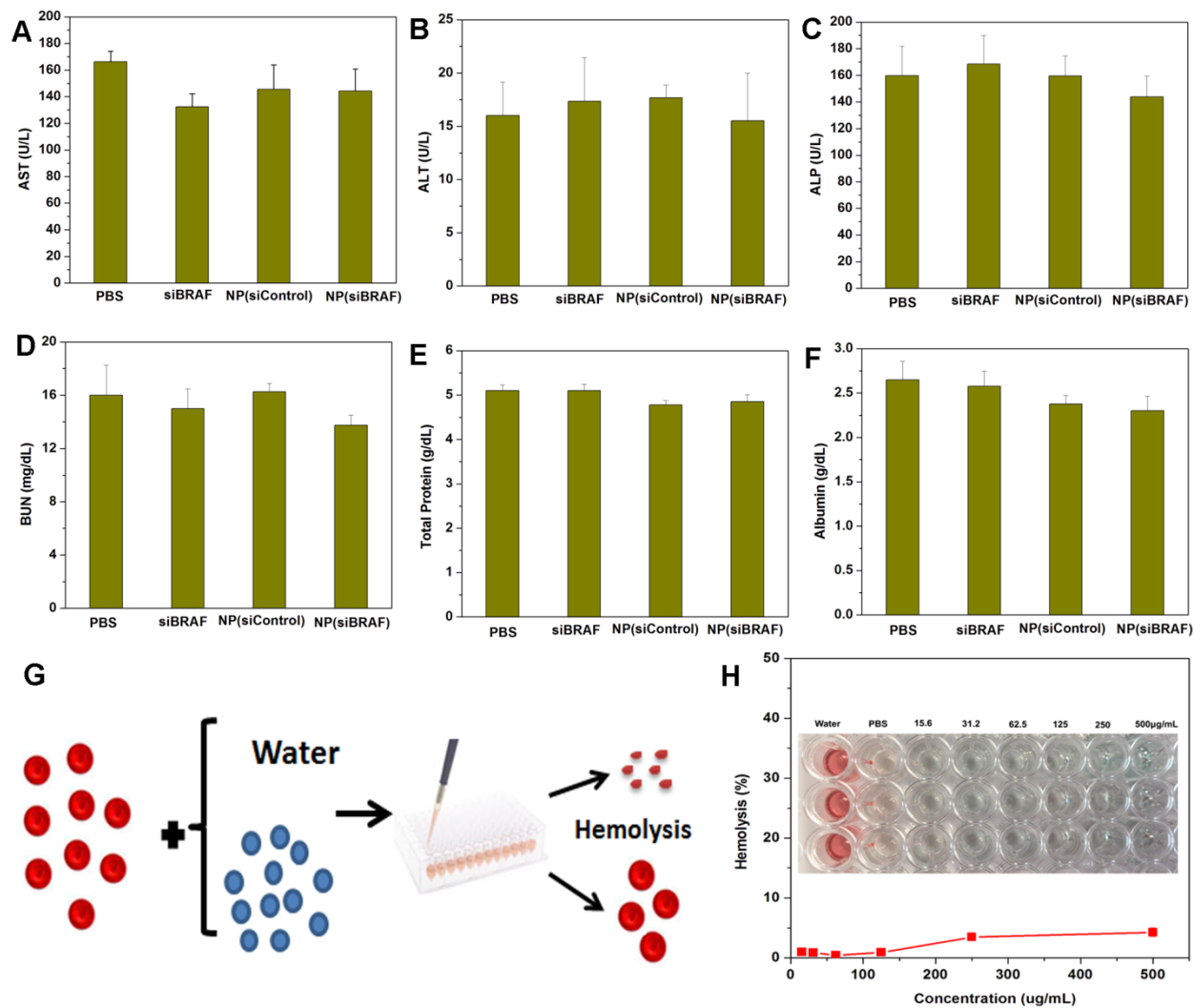


Fig. S14. Investigation of NP toxicity *in vivo*. Serum levels of (A) aspartate aminotransferase (AST), (B) alanine aminotransferase (ALT), (C) alkaline phosphatase (ALP), (D) blood urine nitrogen (BUN), (E) total protein (TP), and (F) albumin after three daily IV injections of saline, naked siBRAF, NP(siControl), or NP(siBRAF). (G,H) Blood compatibility evaluation of NP(siBRAF).

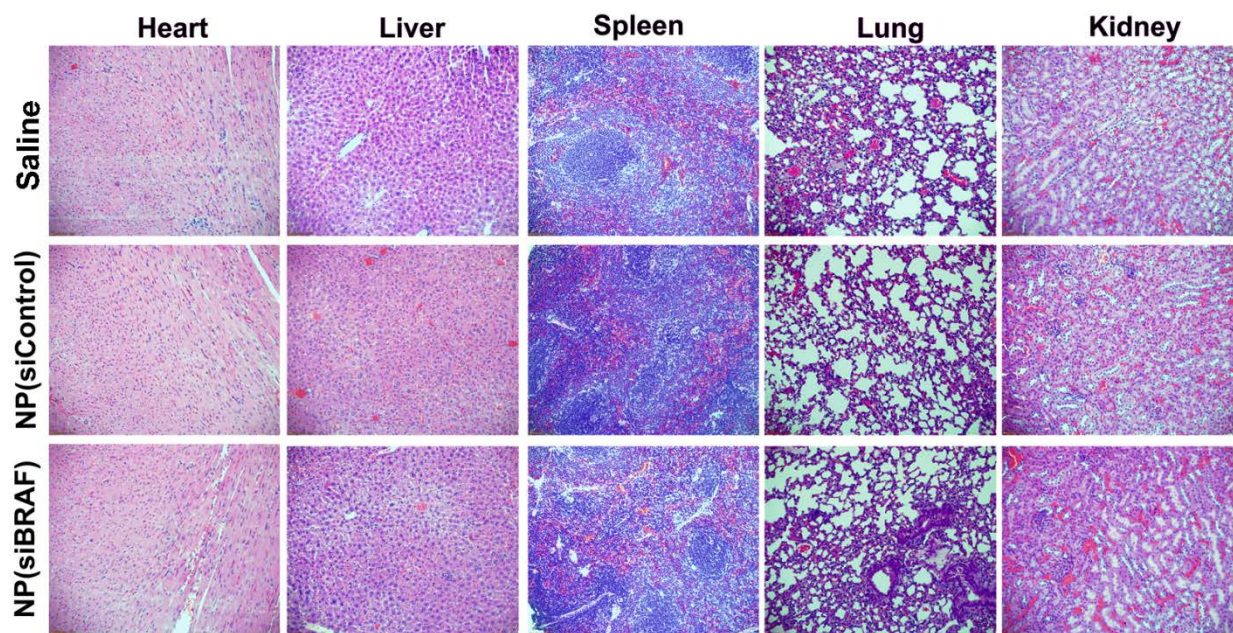


Fig. S15. Representative hematoxylin and eosin (H&E) stained histological images of tissue sections from major organs after treatment with NP(siControl), NP(siBRAF), or saline. Images were taken under 20× objective.

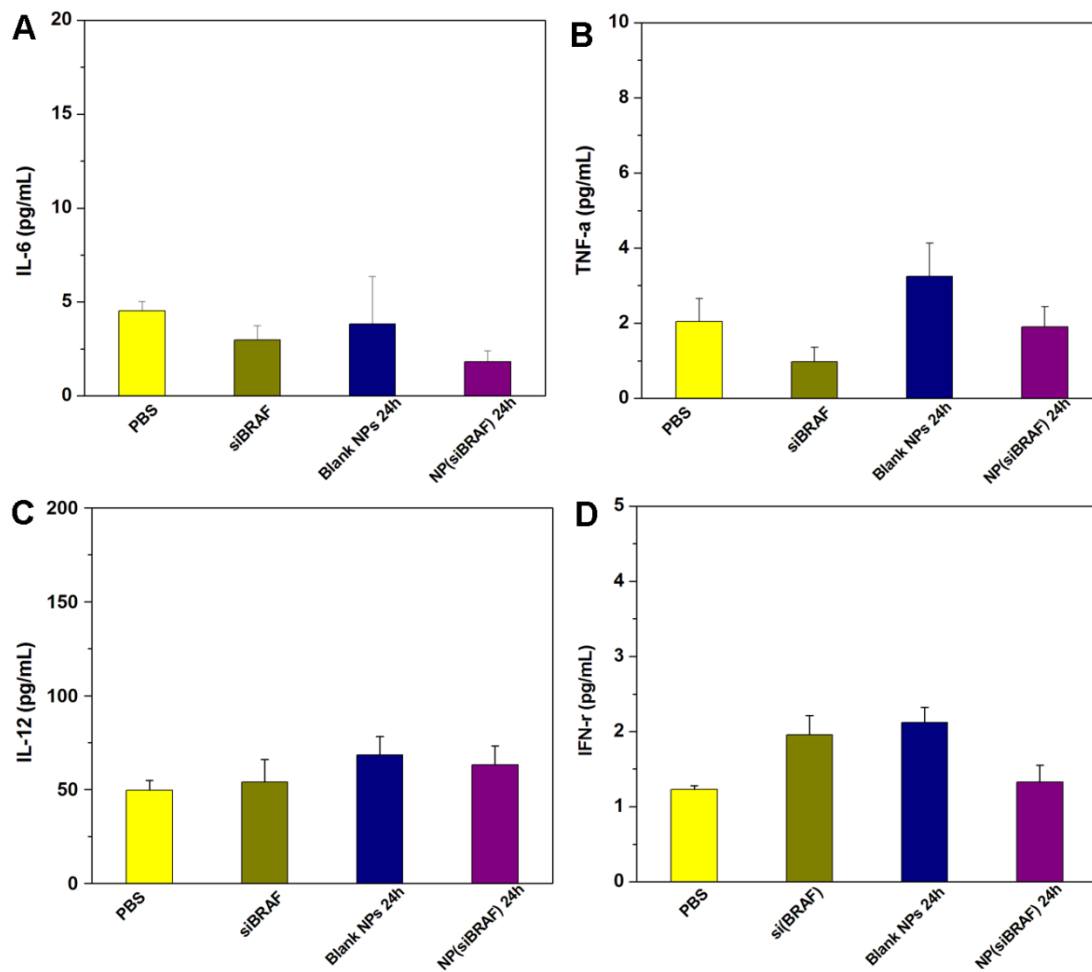


Fig. S16. Immune response after NP treatment. Serum levels of (A) IL-6, (B) TNF- α , (C) IL-12, and (D) IFN- γ 24 h after IV injection of saline, naked siBRAF, blank NP, or NP(siBRAF).

Table S1. siRNA sequences used in this work.

siRNA	Sequence (sense strand, from 5'-end to 3'-end)
Luciferase	CUUACGCUGAGUACUUCGAdTdT
DY647-siRNA	Dy647-labeled CUUACGCUGAGUACUUCGAdTdT
BRAF#1	CAU GAA GAC CUC ACA GUA AUU
BRAF#2	UCA GUA AGG UAC GGA GUA AUU
BRAF#3	AGA CGG GAC UCG AGU GAU GUU
BRAF#4	UUA CCU GGC UCA CUA ACU AUU

Supplemental References

1. Xu, X. *et al.* (2013) Enhancing tumor cell response to chemotherapy through nanoparticle-mediated codelivery of siRNA and cisplatin prodrug. *Proc Natl Acad Sci USA*. 110(46): 18638-18643.
2. Nucera, C. *et al.* (2009) A novel orthotopic mouse model of human anaplastic thyroid carcinoma. *Thyroid* 19(10):1077-1084.